

Determination of Structure and Energetics for Gibbs Surface Adsorption Layers of Binary Liquid Mixture 1. Acetone + Water

Hua Chen,[†] Wei Gan,[†] Bao-hua Wu,[†] Dan Wu,^{†,‡} Yuan Guo, and Hong-fei Wang*

State Key Laboratory of Molecular Reaction Dynamics, Institute of Chemistry, Chinese Academy of Sciences, Beijing, P.R. China 100080

Received: January 11, 2005; In Final Form: February 27, 2005

The orientation, structure, and energetics of the vapor/acetone–water interface are studied with sum frequency generation vibrational spectroscopy (SFG-VS). We used the polarization null angle (PNA) method in SFG-VS to accurately determine the interfacial acetone molecule orientation, and we found that the acetone molecule has its C=O group pointing into bulk phase, one CH₃ group pointing up from the bulk, and the other CH₃ group pointing into the bulk phase. This well-ordered interface layer induces an antiparallel structure in the second layer through dimer formation from either dipolar or hydrogen bond interactions. With a double-layer adsorption model (DAM) and Langmuir isotherm, the adsorption free energies for the first and second layer are determined as $\Delta G^{\circ}_{\text{ads},1} = -1.9 \pm 0.2$ kcal/mol and $\Delta G^{\circ}_{\text{ads},2} = -0.9 \pm 0.2$ kcal/mol, respectively. Since $\Delta G^{\circ}_{\text{ads},1}$ is much larger than the thermal energy $kT = 0.59$ kcal/mol, and $\Delta G^{\circ}_{\text{ads},2}$ is close to kT , the second layer has to be less ordered. Without either strong dipolar or hydrogen bonding interactions between the second and the third layer, the third layer should be randomly thermalized as in the bulk liquid. Therefore, the thickness of the interface is not more than two layers thick. These results are consistent with previous MD simulations for the vapor/pure acetone interface, and undoubtedly provide direct microscopic structural evidences and new insight for the understanding of liquid and liquid mixture interfaces. The experimental techniques and quantitative analysis methodology used for detailed measurement of the liquid mixture interfaces in this report can also be applied to liquid interfaces, as well as other molecular interfaces in general.

1. Introduction

Gibbs and Langmuir laid out the basis for thermodynamic treatment and structural understanding of the structure and energetics of free liquid and liquid mixture interfaces in 1875 and 1917, respectively.^{1–3} Even though surface and colloidal chemistry have found great applications in various chemical, food, and pharmaceutical industries, based on the knowledge accumulated over the decades after applying Gibbs and Langmuir's ground breaking ideas,^{4–6} the lack of effective methods for probing molecular detail of liquid and liquid mixture interfaces has kept us from better microscopic understanding of the chemically and biologically important phenomena at these interfaces, even for the simplest systems, until very recently.^{7–9} Recent progress on intensive experimental,^{7,8,10–15} theoretical,^{16,17} and simulation and computational^{18–24} studies of liquid and liquid mixture interfaces have provided much promise for better detailed microscopic understanding of the vapor/liquid and liquid/liquid interfaces, especially for the aqueous interfaces.²⁵ Comparison between experimental and theoretical simulations for benchmark molecular systems has been conducted intensively.^{9,12,23,26–30} However, the liquid interface is still a very elusive entity, being generally considered dynamic, disordered, and small, and it is still difficult for direct experimental measurement and accurate simulation of their structure and energetics.^{6,9,24,31}

The promises of direct experimental measurement of liquid interfaces and of discerning their structure and energetics at the molecular and microscopic detail dawned upon the development of the nonlinear optical spectroscopic techniques, such as the surface second harmonic (SHG) and sum frequency generation vibrational spectroscopy (SFG-VS), since the early 1980s, for SHG and SFG-VS are nonintrusive and with unique submonolayer sensitivity and interface specificity.^{7,8,32,33} SFG-VS is especially promising because it is the only technique that can yield a vibrational spectrum for molecules at a free liquid or liquid mixture interface,⁸ and it is common knowledge in chemistry and biology that molecular vibrational spectra can be directly related to molecular structure, conformation, and energetics of molecular species. However, obstacles for accurate spectral assignment and quantitative interpretation of the SFG-VS and SHG data have persisted until very recently, and this situation has been holding the progress for further applications of SFG-VS and SHG as the quantitative and accurate interface probing techniques.^{34,35} There has been a continuous and systematic effort for trying to remove such obstacles and to improve the capability of accurate and quantitative applications of SFG-VS and SHG techniques by many research groups,^{36–43} including progress in our laboratory most recently.^{44–49}

Based on the ideas pioneered by Shen, Hirose, and Eiseenthal et al.,^{35,38–41} we have developed quantitative orientational and polarization analysis methodologies with SHG and SFG-VS for interfaces with macroscopic symmetry of $C_{\infty v}$, i.e., rotationally isotropic around the interface normal.^{44–48} In this and a series of following reports we shall show that these developments are particularly useful for detailed analysis of the structure, conformation, and energetics of the free liquid and liquid mixture interfaces. We have shown and shall continue to show that these

* To whom correspondence should be addressed. E-mail: hongfei@mrclab.icas.ac.cn. Tel. 86-10-62555347; Fax 86-10-62563167.

[†] Also graduate students of the Graduate school of the Chinese Academy of Sciences.

[‡] Also research intern at Institute of Chemistry, and undergraduate student at the Department of Chemical Physics, University of Science and Technology of China, before July 2004.

advancements are not only merely simplification with better mathematical formulations but also imply conceptual significance in exploring the capability of SHG and SFG-VS on ordered molecular systems.^{44,47} Some of the key developments are summarized in the following in particular.

(a) SHG and SFG intensity from a $C_{\infty v}$ interface in any particular polarization configuration can be expressed in the following form.^{35,44,46}

$$I(\omega) = \frac{8\pi^3 \omega^2 \sec^2 \beta}{c^3 n_1(\omega) n_1(\omega_1) n_1(\omega_2)} |\chi_{\text{eff}}^{(2)}|^2 I(\omega_1) I(\omega_2) \quad (1)$$

$$\chi_{\text{eff}}^{(2)} = N_s d \langle (\cos \theta) - c \langle \cos^3 \theta \rangle \rangle = N_s d r(\theta) \quad (2)$$

$$I(\omega) = A d^2 R(\theta) N_s^2 I(\omega_1) I(\omega_2) \quad (3)$$

$$R(\theta) = |r(\theta)|^2 = |\langle \cos \theta \rangle - c \langle \cos^3 \theta \rangle|^2 \quad (4)$$

Equation 1 is the general expression for the SFG-VS intensity as known in the literature. SHG is the degenerated case for SFG, so these expressions also stand for SHG with minor differences of constants.^{35,44} Equations 2, 3, and 4 are from our recent developments.^{44,46,47} In eq 1, ω , ω_1 , and ω_2 are the frequencies of the SF signal, visible laser beam, and IR laser beam, respectively. The term $n_i(\omega_i)$ is the refractive index of bulk medium i at frequency ω_i , and $n'(\omega_i)$ is the effective refractive index of the interface layer at ω_i . β_i is the incident or reflection angle from interface normal of the i th light beams; $I(\omega_i)$ is the intensity of the SFG signal or the input laser beams, respectively. The notations and the experimental geometries were described in detail previously.^{35,46} We have shown that $\chi_{\text{eff}}^{(2)}$ could be simplified into eq 2 for interfaces with macroscopic symmetry of $C_{\infty v}$, i.e., rotationally isotropic around the interface normal.^{44,46} We also pointed out that a general formulation for treatment on linear and nonlinear susceptibilities of ordered monolayers, as well as ordered molecular films, with coherent and incoherent linear and nonlinear optical techniques can also be similarly formulated.⁴⁷

In eq 2, N_s is interface molecular number density, θ is the tilting angle between the molecular main (z') axis and the interface normal (z axis) in the laboratory coordinates, $r(\theta)$ is called the "orientational field functional", which contains all molecular orientational information at a given SFG experimental configuration; while the dimensionless parameter c is called the "general orientational parameter", which determines the orientational response $r(\theta)$ to the molecular orientation angle θ ; and d is the susceptibility strength factor, which is a constant in a certain experimental polarization configuration with a given molecular system. The d and c values are both functions of the related Fresnel coefficients, including the refractive index of the interface and the bulk phases, and the experimental geometry. Both d and c could be derived from the expressions of the $\chi_{\text{eff}}^{(2)}$ in relationship to the macroscopic susceptibility and microscopic (molecular) hyperpolarizability tensors for a particular molecular (microscopic) symmetry.^{44,46}

In eq 3, A is an experimental constant. It is clear that the SFG intensities for different experimental configurations are clearly parametrized in eq 3, and the term $d^2 R(\theta)$, $r(\theta)$ combined or separately, plays a central role in quantitative polarization and orientation analysis of the SFG and SHG experiments.^{44,46} More comprehensive discussions of the advantages, details for analysis, and possible applications in SHG and SFG with such a formulation was presented in our previous works.^{44,46}

(b) With the formulation in (a), polarization selection rules for vibrational spectral analysis in SFG-VS have been derived for molecular groups with different molecular (microscopic) symmetries, using the C–H stretching vibrational modes for methyl (C_{3v}), methylene (C_{2v}), and methine ($C_{\infty v}$) groups as working examples.^{46,48} C–H stretching vibrational modes have been complex and difficult in IR and Raman spectroscopy.^{50–54} With these polarization selection rules, not only have clear and unambiguous assignment of the SFG-VS spectra for C–H stretching vibrational modes been achieved, but also quite a few issues in the previous IR, Raman, and SFG-VS spectral assignments were clarified.^{46,48} From these applications, it has been shown that the formulation is very effective for solving problems in polarization and orientation analysis with SFG-VS. It is because the SHG and SFG-VS are coherent polarization spectroscopic methods, and interfaces are preferentially oriented molecular systems. The polarization selection rules and polarization analysis of other molecular groups and symmetries can be worked out similarly. This development could significantly help the applications of SFG-VS for more complex molecular interfaces, such as polymer films and biomembranes.

(c) With eq 4, it is clear that when $R(\theta) = 0$, $c_0 = D = \langle \cos \theta \rangle / \langle \cos^3 \theta \rangle$. Therefore, the orientational parameter D could be accurately measured with the polarization null angle (PNA) method.^{44,45,49} Because $\chi_{\text{eff}}^{(2)}$ can be expressed as the linear combination of the $\sin \Omega$ and $\cos \Omega$ terms, in PNA, a polarization angle Ω_{null} for the SF signal satisfies a zero (null) value of the SF intensity, i.e., $I(\omega) \propto |\sin(\Omega - \Omega_{\text{null}})|^2 = 0$, when the polarization angle for visible (Ω_1) and IR (Ω_2) are at fixed values, usually with $\Omega_1 = 0$ and $\Omega_2 = 45^\circ$ or -45° .⁴⁵ Using this accurately measured Ω_{null} value, a D value can be explicitly calculated with the known experimental configuration parameters.^{44,45,49} Thus, the determined D value has a high accuracy, even for the case when the widely used intensity ratio between two different polarizations, usually with $I_{\text{ssp}}(\omega)/I_{\text{sps}}(\omega)$, failed to have a certain value when $I_{\text{sps}}(\omega)$ is close to the noise level.^{44,45} Here s is defined as the polarization perpendicular to the incident plane; and p is polarization in the incident plane. The symbol ssp indicates that the SF, visible, and IR beams are polarized in s , s , p directions, respectively, and so on. We have shown that with PNA, as well as with the general formulation of the orientational parameter D ,⁴⁹ the orientational tilt angle θ for the CH_3 groups at vapor/methanol and vapor/acetone interfaces can be determined accurately.^{45,49} This development not only provides a direct measurement of the interface structure and conformation, but also provides a way to decouple the orientational contribution $R(\theta)$ and surface density N_s in eq 3, ensuring detailed structural and energetics analyses of the Gibbs adsorption thermodynamics.

A particularly important issue in above quantitative polarization and orientational analysis is what is the value for the effective dielectric constant, i.e., microscopic local field factors, in the interface layer.^{35,44–46} A general treatment of the microscopic local field factors in a polarizable two-dimensional molecular layer adsorbed on metal interface was formulated by Ye and Shen in 1983.⁵⁵ Recently, a formulation for the simple liquid interface based on a modified Lorentz model was also described by Shen et al.³⁵ These two treatments agree well for simple liquid interfaces under the nonresonant conditions because the value of the linear molecular polarizability is usually small. The problem and consequences of the microscopic local field corrections in SHG and SFG-VS can also be explicitly addressed with the formulation in (a). We shall report this elsewhere. Without much further ado, we will follow the

modified Lorentz model in our SFG-VS treatment of the liquid interfaces, which has been successfully applied to SFG-VS so far.^{35,45,46,48}

We shall show in this report that a general approach in SFG-VS based on the above developments can be used to obtain detailed information on the structure and energetics of the Gibbs surface layers at the vapor/acetone–water mixture interface. First, we shall use the PNA method to determine the orientation of acetone molecule at the interface at various acetone concentrations. Second, by separating the contributions from the orientation and surface density, we shall identify the two-layer structure of the vapor/acetone–water mixture interface. Finally, we use a double-layer adsorption model (DAM) and Langmuir isotherm to obtain the adsorption free energies of the acetone molecule for the first and second layer adsorptions. Our findings show that the acetone molecules are well ordered in the first layer, and this layer induces a partially ordered second layer with an antiparallel structure. This structure should prevent the formation of the third layer, which is already fully thermalized as part of the bulk phase. The adsorption free energies for the two adsorption layers are $\Delta G^{\circ}_{\text{ads},1} = -1.9 \pm 0.1$ kcal/mol and $\Delta G^{\circ}_{\text{ads},2} = -0.9 \pm 0.2$ kcal/mol, respectively. $\Delta G^{\circ}_{\text{ads},2}$ is not much bigger than the thermalization energy $kT = 0.59$ kcal/mol at the ambient temperature of 295 K. Therefore, the second layer can only be partially ordered, i.e., not as ordered as the first layer. This is the first time such detailed information has been directly obtained for any liquid or liquid mixture interface, and it opens the door for further understanding of the important issues for liquid interface in general.

2. Experimental Section

Our picosecond SFG-VS spectrometer was from EKSPLA, and it has been described in detail previously.⁴⁶ Briefly, the 10 Hz and 23 picosecond SFG spectrometer laser system is using a co-propagating configuration. Some of the SFG polarization optics were rearranged from the original design by EKSPLA to improve the polarization control in the SFG experiment.⁴⁵ The visible wavelength is fixed at 532 nm and the full range of the IR tunability is 1000 cm^{-1} to 4300 cm^{-1} . The incident angles are $\beta_1 = 62^\circ \pm 1^\circ$ for the visible beam, and $\beta_2 = 52^\circ \pm 1^\circ$ for the IR beam. The SFG signal is collected around 60.5° (β) at the reflection geometry, within a small range (about 0.3°) which depends on the corresponding IR wavelength tuning range (from 2800 to 3000 cm^{-1} in the experiment). Each scan was with a 2 cm^{-1} increment and was averaged over 100 laser pulses per point. The energy of visible beam is typically less than 300 microjoules and that of IR beam less than 200 microjoules. So the intensity in our experimental conditions cannot damage or cause any heat effect and other photochemical reactions to the liquid samples. The spectrum intensity is normalized to the intensities of the corresponding visible and IR laser pulses.

The PNA experiments were performed at the peak of the CH_3 symmetric stretching mode of the SFG-VS spectra at each concentration. The polarization of the IR beam is kept at p polarization, and the polarization angle of the visible beam is -45° (positive sign is clockwise when facing the coming direction of the beam).⁴⁵

Particular attention has to be paid to accurate control of the polarizations in PNA experiment. We have found that in the SFG optical arrangements of the original design for the EKSPLA SFG spectrometer, the polarization of the visible beam is purely linear only for s or p polarizations. This optical arrangement is fine for measurement only with the ssp, ppp, sps, and pss polarization combinations. It had not been an issue because the

TABLE 1: Values of c and d for the CH_3 -ss Mode of Vapor/Acetone–Water Mixture Interface in Different Polarization Configurations

polarization	c	d
ssp	−0.306	$0.344 \beta_{\text{ccc}}^{(2)}$
ppp	1.491	$0.176 \beta_{\text{ccc}}^{(2)}$
sps	1	$-0.122 \beta_{\text{ccc}}^{(2)}$
pss	1	$-0.119 \beta_{\text{ccc}}^{(2)}$

general practice in the SFG-VS has not gone beyond these four polarization combinations until very recently,^{44,45} and the majority of the works deals only with the ssp or ppp polarization combination. However, in this EKSPLA design, any polarization other than s or p for the visible beam is somewhat elliptical. This certainly gives incorrect null angle values when the visible polarization angle is set at $\Omega_1 = -45^\circ$. We have found out that simple adjustment of a few optical components for polarization control of the visible beam can correct the problem.⁴⁵ We have made the due adjustment for all our experiments since. Any laboratory who has been using the complete EKSPLA SFG spectrometer system is suggested to take notice if they plan to perform any measurement with visible light polarization other than s and p. Comparisons of the existing results with such measurements have to be cautiously taken.

All measurements were carried out at controlled room temperature ($22.0 \pm 0.5^\circ\text{C}$). The liquid acetone is GC grade from Fluka (99.5%), used without further treatment. Doubly distilled water was prepared with Millipore Simplicity 185 (18.2 M $\Omega \cdot \text{cm}$). The liquid sample is filled in a round Teflon beaker (diameter ~ 5 cm) for SFG measurement. The whole experimental setup on the optical table was covered in a plastic housing to reduce the air flow and the evaporation.

3. Results and Discussion

3.1. SFG-VS Spectra and Orientation of the Vapor/Acetone–Water Mixture Interface. The SFG-VS spectra of the CH_3 group between 2800 cm^{-1} and 3000 cm^{-1} were obtained for vapor/neat acetone interface in ssp, ppp, sps, and pss polarization configurations,^{29,35,49} and vapor/acetone–water interface at 0.1 mole fraction previously.⁵⁶ The d and c values for this ss mode in the four polarizations in our experimental condition are listed in Table 1, calculated from the following parameters: $n_1(\omega_{\text{vis}}) = 1.0$, $n_1(\omega_{\text{IR}}) = 1.0$, $n_1(\omega_{\text{SF}}) = 1.0$, $n_2(\omega_{\text{vis}}) = 1.359$, $n_2(\omega_{\text{IR}}) = 1.349$, $n_2(\omega_{\text{SF}}) = 1.359$, $n'(\omega_{\text{vis}}) = 1.160$, $n'(\omega_{\text{IR}}) = 1.156$, $n'(\omega_{\text{SF}}) = 1.160$, and hyperpolarizability tensor ratio $R = \beta_{\text{aac}}^{(2)}/\beta_{\text{ccc}}^{(2)} = 1.881$.^{29,48,49} Since the refractive index of water at room temperature is $n_{\text{water}} = 1.333$, therefore, the refractive indexes of acetone/water mixture for different acetone concentrations are nearly the same, so in all the calculations we will use the same refractive index values listed above. It is easy to show from $d^2R(\theta)$ values that the intensity on ssp spectra should be 20 times stronger than those of the ppp, sps, and pss spectra. This well exemplifies the polarization selection rules for the CH_3 -ss mode in SFG-VS spectra.

Systematic SFG-VS study on vapor/acetone–water mixture interfaces has not been reported before, except for ssp spectra at 0.1 mole fraction.⁵⁶ At different bulk concentrations, the SFG-VS spectra show a single recognizable peak around 2920 cm^{-1} on the ssp polarization, fully in accordance with the $d^2R(\theta)$ values above. Therefore, in Figure 1 we presented only the ssp SFG-VS spectra at four typical bulk mixture concentrations. In Table 2, however, we listed the single peak Lorentzian fitting parameters of the ssp spectra with eq 6 for all the bulk mixture

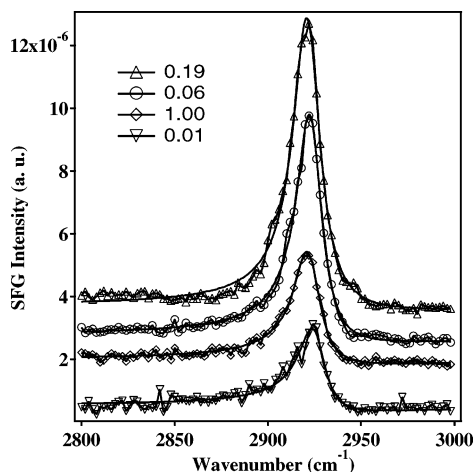


Figure 1. SFG-VS ssp spectra in the C–H stretching region at different bulk acetone concentrations. ∇ : 0.01, \circ : 0.06, \triangle : 0.19, and \diamond : 1.00. The solid lines are fitted lines with Lorentzian and the short lines are connection between neighboring points.

concentrations we have measured. In fitting the spectra, we have^{8,35,46}

$$I(\omega_{\text{IR}}) = C + B^* |\chi_{\text{nr,eff}}^{(2)} + \chi_{\text{r,eff}}^{(2)}(\omega_{\text{IR}})|^2 \quad (5)$$

$$= C + B^* \left| \chi_{\text{nr,eff}}^{(2)} + \frac{A_{q,\text{eff}}}{\omega_{\text{IR}} - \omega_q + i\Gamma_q} \right|^2 \quad (6)$$

$$A_{q,\text{eff}} \propto d_{q,\text{eff}} r(\theta) N_{\text{s,eff}} \quad (7)$$

in which $\chi_{\text{nr,eff}}^{(2)}$ and $\chi_{\text{r,eff}}^{(2)}$ are the nonresonant and resonant contributions to the SFG-VS susceptibility $\chi_{\text{eff}}^{(2)}$, respectively. $A_{q,\text{eff}}$, ω_q and Γ_q are the oscillator strength, resonant frequency and damping constant of the q th vibrational mode. B and C are two fitting constants. Therefore, the oscillator strength $A_{q,\text{eff}}$ should be proportional to the intensity factor $d_{q,\text{eff}}$ for the q th vibrational mode, orientational functional $r(\theta)$, and the interfacial density $N_{\text{s,eff}}$ in SFG-VS. It is important to note that the $d_{q,\text{eff}}$ and c values used to calculate the $A_{q,\text{eff}}$ values are dependent on the Fresnel factors at the interface, and these Fresnel factors will not be constant at different bulk concentrations if the two liquids under mixing have very different bulk refractive indexes. However, for acetone and water, their bulk refractive indexes are close enough to each other, so it is valid that we use the same $d_{q,\text{eff}}$ and c values throughout the whole bulk concentration range.

We measured the null angle $\Omega_{\text{SF}}^{\text{null}}$ at the CH_3 -ss peak position at each different bulk mixture concentration using the PNA method, and calculated the corresponding orientational parameter $D = \langle \cos \theta \rangle / \langle \cos^3 \theta \rangle$ at each concentration with the relationship in eq 8.^{45,44,49} These results are also listed in Table 2.

$$D = \frac{\langle \cos \theta \rangle}{\langle \cos^3 \theta \rangle} = \frac{0.176 \times 1.491 + 0.344 \times 0.306 \tan \Omega_{\text{SF}}^{\text{null}}}{0.176 - 0.344 \tan \Omega_{\text{SF}}^{\text{null}}} \quad (8)$$

From the data in Table 2 and existing literature in the field, the following observations could be made.

(a) In Table 2, the spectra peak position red-shifted about 4 cm^{-1} from 0.01 bulk mole fraction (very dilute acetone aqueous solution) to 1.00 bulk mole fraction (pure acetone), with the HWHM almost unchanged. Similar red shifts were reported for the CH_3 -ss SFG-VS spectra of vapor/methanol–water mixture interfaces, as well as for the Raman and FTIR spectra of bulk methanol–water mixture, by Allen et al. previously.⁵⁷ This red-shift was attributed to the changing hydrogen bonding configuration between the methanol and water molecules at the surface and in the bulk.

(b) In Table 2, the SFG-VS spectral peak intensity for CH_3 -ss is strongest between mole fraction at 0.14 and 0.19, and it dropped about 60% at 1.00 mole fraction, so the calculated oscillator strength dropped about 40%. Similar but different percentages of drops for the SFG-VS intensity of the CH_3 -ss peak in ssp spectra with increasing bulk concentration were also reported for other vapor/aqueous solution mixtures such as methanol–water (about 30% of intensity at room temperature),^{57,58} acetonitrile–water (about 50% of intensity at room temperature),⁵⁹ ethanol–water (about 50% of intensity at room temperature),⁶⁰ and most recently acetic acid–water (about 50% of CH_3 -ss and about 80% of the C=O symmetric stretching intensity at 4°C)⁶¹ mixtures. Allen et al. have carefully pointed out that the IR absorption of the methanol vapor close to the liquid sample cell at room temperature is less than 5%.⁵⁷ Therefore, the drop of the SFG-VS intensity is real and cannot be attributed to such experimental artifact. In our experiment, we also made sure that the vapor absorption of the IR energy was not causing problems for the SFG intensity drop. We found out that to perform the SFG-VS experiment in an open beaker is ideal.

However, in the literature, the interpretations for the SFG-VS intensity decrease phenomenon with increasing bulk concentration were very different in different works. In the methanol and acetonitrile cases,^{57–59} the decrease of SFG intensity at higher bulk concentration was attributed to the decrease of the interface ordering at higher bulk concentration, because the number of adsorbed methanol or acetonitrile molecules in the interface region has to increase with bulk concentration. However, without direct measurement of molecular orientation at those interfaces, these interpretations still cannot be put on a very solid ground. While for the ethanol and acetic acid cases,^{60,61} SFG spectra intensity ratio between two different polarizations suggested that the interface ordering did not change much with bulk concentration. So the drop of the SFG-VS intensity was attributed to possible increase of the interface

TABLE 2: Fitting Parameters for SFG-VS Spectra of CH_3 -ss of Vapor/Acetone–Water Mixture Interfaces

mole frac	peak (cm^{-1})	HWHM (cm^{-1})	$A_{q,\text{eff}}$ (a.u.)	$\Omega_{\text{SF}}^{\text{null}}$ (deg)	D
0.01	2925.4 ± 1.6	7.7 ± 0.2	0.0070 ± 0.0010	-8.4 ± 1.6	1.09 ± 0.06
0.03	2923.8 ± 0.7	8.4 ± 0.6	0.0120 ± 0.0020	-9.7 ± 1.2	1.04 ± 0.04
0.06	2923.0 ± 0.7	8.3 ± 0.6	0.0146 ± 0.0009	-10.0 ± 1.0	1.03 ± 0.03
0.14	2922.1 ± 0.2	8.6 ± 0.6	0.0170 ± 0.0010	-11.1 ± 1.0	0.99 ± 0.03
0.19	2921.5 ± 0.3	9.2 ± 0.5	0.0170 ± 0.0007	-12.2 ± 1.0	0.96 ± 0.03
0.36	2921.1 ± 0.7	8.7 ± 0.7	0.0140 ± 0.0010	-12.9 ± 1.0	0.93 ± 0.03
0.50	2921.1 ± 0.9	8.3 ± 0.7	0.0119 ± 0.0007	-14.3 ± 2.4	0.89 ± 0.06
0.69	2921.0 ± 0.3	7.7 ± 0.7	0.0102 ± 0.0010	-16.7 ± 1.1	0.83 ± 0.04
0.86	2921.3 ± 0.9	7.9 ± 0.6	0.0098 ± 0.0008	-16.5 ± 1.0	0.83 ± 0.03
1.00	2921.5 ± 1.4	8.1 ± 0.5	0.0095 ± 0.0007	-16.5 ± 1.5	0.83 ± 0.05

TABLE 3: Calculated Orientational Angles for Acetone Molecule at the Vapor/Acetone–Water Mixture Interfaces

mole frac	D	$\theta\text{-CH}_3^1$ (deg)	$\theta\text{-CH}_3^2$ (deg)	$\theta\text{-C=O}$ (deg)	error bar (deg)
0.01	1.09 ± 0.06	-23.0	94.2	-144.4	2.1
0.03	1.04 ± 0.04	-21.7	95.5	-143.1	1.8
0.06	1.03 ± 0.03	-21.4	95.8	-142.8	1.6
0.14	0.99 ± 0.03	-20.3	96.9	-141.7	1.7
0.19	0.96 ± 0.03	-19.1	98.1	-140.5	1.7
0.36	0.93 ± 0.03	-18.4	98.8	-139.8	1.7
0.50	0.89 ± 0.06	-16.8	100.4	-138.2	2.1
0.69	0.83 ± 0.04	-14.1	103.1	-135.5	1.8
0.86	0.83 ± 0.03	-14.1	102.8	-135.8	1.7
1.00	0.83 ± 0.03	-14.1	102.8	-135.8	1.9

ethanol concentration for one case and to possible antiparallel double layer formation at low temperature for the acetic acid case. These results and interpretations are on better ground with intensity ratio data for orientational analysis, especially for the SFG study on the vapor/acetic–acid mixture interface, but the conclusions are still qualitative before direct quantitative measurement of the molecular orientation and orientational change at the interfaces can be made.

(c) In Table 2, the measured null angle of the $\text{CH}_3\text{-ss}$ peak on the SFG-VS spectra and the calculated orientational parameter D clearly show a monotonic increase of the interface order. It shows that as the acetone bulk concentration increases from 0.01 to 1.00 mole fraction, the measured D value decreases from 1.09 ± 0.06 to 0.83 ± 0.06 . The relationship between the interface orientational order and the D value has been extensively discussed in recent years.^{44,45,49,62,63} It is known that when D is close to 1, the smaller the D values, the better the orientation order and the narrower the orientational distribution.^{44,62,63} However, for each acetone molecule there are two methyl groups. With a narrow orientational distribution, these two methyl groups should have distinctive orientation angles. To solve this problem, a new method was recently developed in our group for determination of the orientational angles for both CH_3 groups in an interfacial acetone molecule.⁴⁹ Providing the MeCMe plane of the acetone molecule is perpendicular to the interface,²⁹ the two angles can be determined uniquely through the following relationship:⁴⁹

$$D = \frac{x\langle\cos\theta_1\rangle + (1-x)\langle\cos\theta_2\rangle}{x\langle\cos^3\theta_1\rangle + (1-x)\langle\cos^3\theta_2\rangle} \quad (9)$$

where $\theta_2 = 117.2^\circ + \theta_1$, because the angle between the two CH_3 groups is 117.2° , and $x = 0.5$, because the number of the two CH_3 groups are equal. Table 3 gives the values for the calculated orientational angles with the assumption of the δ orientational distribution. As we have shown elsewhere,⁴⁹ the orientational angular distribution of acetone molecules at the interface with such small D values could not be very broad. We will further discuss the influence of the angular distribution on determination of the Gibbs adsorption energetics below.

The failure to observe the C=O stretch around 1700 cm^{-1} in SFG-VS measurement on the vapor/pure acetone interface was used as an indicator that the C=O group could lie near the interface.²⁹ However, our calculation with the known IR and Raman spectral intensities of the C=O group in acetone showed that with $\theta_{\text{C=O}} = -135.8^\circ \pm 1.9^\circ$, its SFG-VS intensity should be at least more than one order smaller than that of the $\text{CH}_3\text{-ss}$ mode. To our knowledge, observation of the C=O group SFG-VS spectra in acetone has not been reported so far. With a significant improvement of the detection sensitivity of our SFG-VS spectrometer, we have obtained the C=O group SFG-VS

spectra on the ssp polarization around 1720 cm^{-1} for the vapor/acetone–water mixture interface with a bulk mole fraction of 0.4. The intensity is more than 30 times weaker than that of $\text{CH}_3\text{-ss}$, which prevents us from accurate measurement with PNA method of the D value for the C=O group before further improvement of the detection sensitivity of the instrument. Nevertheless, this result clearly indicates that the C=O group of acetone does not seem to lie close to parallel to the interface as previously suggested,²⁹ and this fact indeed suggests that the orientational distribution width for the C=O group is not more than a few degrees.⁴⁹ Therefore, the calculated orientational angles in Table 3 using a δ -distribution function should be acceptable for analysis below.

It is easy to see in Table 3 that the orientational angle of the C=O group, which is parallel to the direction of the permanent dipole, gets more tilted from the interface normal as the bulk acetone concentration increases, i.e., the interface is more crowded with adsorbed acetone molecules. If C=O became more parallel to the interface normal at higher surface density, there would be a bigger dipolar repulsion between the acetone molecules at the interface. Therefore, such configuration may certainly help reduce such energetically unfavorable interaction or be a direct result of such repulsive interaction. It is interesting to see the fact that even though the CH_3 group is hydrophobic and prefers to stick out of the bulk phase, one of the CH_3 groups of acetone actually sticks into the bulk phase, which is certainly more hydrophilic. This suggests that the reduction of the dipolar repulsion must be big enough to compensate the energy increase from this CH_3 configuration. We can further surmise that it is energetically favorable to have the other CH_3 group of the interface acetone molecule stay as far away from the bulk phase as possible. This scenario predicts that the acetone molecule at the interface should have its molecular plane perpendicular to the interface, as predicted from the MD simulation for the pure vapor/acetone interface previously.²⁹ We think that this scenario is highly likely for the vapor/acetone–water mixture interface at high interface acetone densities.

In addition to this dipole repulsion scenario for the higher bulk concentration, the antiparallel dimer formation could also be a possibility. MD simulations have shown that in the bulk acetone liquid, acetone molecules can form dimer structures through nonlinear configuration of hydrogen bonds between the oxygen of one acetone molecule and the hydrogen atom on one of the CH_3 groups of another acetone molecule.⁶⁴ This antiparallel structure can easily explain the fact that at higher concentrations the C=O stretch vibrational spectra could not be detected with SFG at the vapor/pure acetone interface.²⁹ This antiparallel structure is illustrated in Figure 4, and shall be further discussed in next section.

At low interface density, the interactions between acetone and water molecules determine the orientation of the interfacial acetone molecule. The vibrational spectra peak shift above-mentioned is clearly an indication of such change of interactions. As shown by the classical SFG paper by Shen et al.,³⁰ the permanent dipole moment of the interfacial water molecules at the vapor/water interface points into the bulk phase and orients close to parallel to the interface plane. When an acetone molecule is put at the vapor/water interface, the interfacial water dipole would try to pull the acetone dipole away from the interfacial normal, or to pull one of the acetone CH_3 groups to form some kind of hydrogen bond, so that the acetone molecule assumes an energetically more favorable configuration at the interface. As a consequence, one of the CH_3 of acetone molecules could be pulled into the bulk phase, and the molecular

plane of the acetone molecule would be energetically favorable to allow the other CH₃ to stay as far away from the interface as possible, and the molecular plane is to be perpendicular to the interface. In this scenario, it is likely that the attractive interaction between water and acetone dipoles, as well as some kind of the hydrogen bond between the water and acetone molecules, determines the orientation of the acetone molecule; while at higher interface density the scenario above suggests that the repulsion between the acetone dipoles or a antiparallel dimer formation through hydrogen bonding determines the orientation. Both scenarios clearly favor the tilted dipole orientation of the acetone molecule and the acetone molecular plane being perpendicular to the interface.

The above interpretation of the orientation of the acetone molecule is supported with the direct experimental measurement results. However, alternative interpretations might also be possible. We believe that the important thing here is that now it is possible to make such detailed direct measurements on the molecular orientation of the interfacial acetone molecule and watch slight orientational change with changing concentration and other conditions of the interface system. This further allows the possibility for understanding the subtle interplay and detailed balance of the interactions with hydrogen bonding, dipole, and hydrophobic effects at the detailed molecular level of the liquid interface.¹⁹

We would like to point out that such direct measurement of the molecular orientation of a vapor/liquid mixture interface at different bulk concentrations has not been done before. It has not been possible without the application of the SFG-VS PNA method, which allows accurate measurement of the SFG-VS null angle and allows the comparison of the slight orientational changes with small changes in the orientational parameter D for a molecular groups at the interface. Such an accuracy was certainly unattainable with the intensity ratio method generally used in the literature.^{60,61,65,66} It was also not possible to use the intensity ratio method for molecular groups that only have measurable SFG intensity in the ssp polarization. Therefore, experimental determination of molecular orientation of some of the most important liquid interfaces, such as the vapor/acetone, vapor/methanol, and vapor/acetonitrile interfaces, were not achieved.^{29,57,59,65,67,68} The advantages of the PNA methods were fully discussed in our recent report,^{44,45,49} and here is a clear demonstration of its usefulness for providing new tools and new insights for understanding the structure and energetics of molecules at interfaces.

3.2. The Antiparallel Double Layer Structure and Energetics of the Vapor/Acetone–Water Mixture Interface. With the detailed knowledge of the orientation of the acetone molecules, we shall establish below the existence of an antiparallel double layer adsorption structure at the vapor/acetone–water interface and demonstrate that the energetics for the Gibbs adsorption layers can be determined.

With the orientational angle obtained above, it is now possible to calculate the interfacial effective molecular density $N_{s,eff}$. From the definition of the orientational functional $r(\theta)$ and with the consideration of the fact that there are two distinctively oriented CH₃ groups, $r(\theta)$ for the ssp polarization can be calculated through eq 10.

$$r(\theta) = (\langle \cos\theta_1 \rangle + \langle \cos\theta_2 \rangle) - c_{ssp} (\langle \cos^3\theta_1 \rangle + \langle \cos^3\theta_2 \rangle) \quad (10)$$

where $c_{ssp} = -0.306$ as listed in Table 1. The only assumption here is that the two methyl groups in an acetone molecule are identical except for their orientational angles. The calculated $r(\theta)$ values for different bulk concentration are listed in Table

TABLE 4: Calculated Interfacial Orientational Functional, Effective CH₃ Group Density, and Surface Coverage for the First and the Second Gibbs Adsorption Interfacial Layers at Vapor/Acetone–Water Interfaces

mole frac.	D	$r(\theta)$	$N_{s,eff}$ (a.u.)	Θ	σ
0.00			0.0000	0.00	0.00
0.01	1.09	1.09	0.0061	0.20	0.010
0.03	1.04	1.08	0.0110	0.44	0.058
0.06	1.03	1.08	0.0140	0.62	0.15
0.14	0.99	1.07	0.0160	0.80	0.36
0.19	0.96	1.06	0.0160	0.86	0.48
0.36	0.93	1.06	0.0130	0.93	0.69
0.50	0.89	1.04	0.0110	0.96	0.80
0.69	0.83	1.02	0.0100	0.98	0.90
0.86	0.83	1.02	0.0096	0.99	0.96
1.00	0.83	1.02	0.0093	1.00	1.00

4. $r(\theta)$ changed only a few percent from 1.09 to 1.02 when bulk mole fraction changed from 0.01 to 1.00. This is not surprising for the ssp polarization. For $c_{ssp} = -0.306$, $r(\theta)$ is not a very fast changing function itself. Additionally, the two CH₃ groups orient one up and one down from the interface, and their orientational angles are just in the range that the changes caused by changing orientation cancel each other, thus making the $r(\theta)$ insensitive to orientational changes in a fairly broad range of θ . Furthermore, it is easy to show mathematically that in such a range of θ , even with some orientational angular distribution, the orientationally averaged $r(\theta)$ would not change much. This makes the measurement orientation insensitive in this particular orientational range and with the particular ssp polarization configuration.

Orientation insensitive measurement with SHG was discussed by Simpson and Rowlen previously.⁶⁹ It is a very good concept for obtaining adsorption free energy and adsorption kinetics measurement with improved accuracy, but this idea has not found many applications since. We found out that by using our formulation with the orientational functional $r(\theta)$, it is conceptually easier to formulate and calculate the orientation insensitive measurement configurations. It is straightforward to choose a proper c value for an orientationally insensitive $r(\theta)$ within a certain range of θ for an interface with particular molecular group, i.e., a set of particular microscopic polarizability tensors, in SHG, as well as SFG-VS experiment.⁴⁴ In short, the ssp polarization is a proper orientation insensitive experimental configuration for acetone at its aqueous interface. So the structure and energetics thus obtained are reliable.

For a particular experimental polarization configuration, e.g., ssp, the d value is a constant. So the effective interfacial density of the CH₃ group, i.e., $N_{s,eff}$, can be simply put as a proportional quantity $A_q/r(\theta)$. The calculated $N_{s,eff}$ values are listed in Table 4 and plotted against the acetone–water mixture bulk concentration in Figure 2.

Because the orientational effect on the SFG-VS intensity has been corrected, the drop of approximately 40% of the $N_{s,eff}$ from its maximum in Figure 2 can no longer be attributed to the assumption that the interface layer is more disordered at higher bulk concentration. Given that SFG-VS only probes the interface region where the centrosymmetry is broken, $N_{s,eff}$ is truly an interface quantity and is proportional to the number of CH₃ groups that contribute to the SFG-VS intensity. With the increase of the bulk acetone concentration, it is expected that the interface should be saturated with adsorbed acetone molecules. Therefore, the actual number of acetone molecules cannot decrease with bulk acetone concentration. The only possibility now is that in this interface region at higher bulk contribution some molecules start canceling the contribution to the SFG signal of the well-

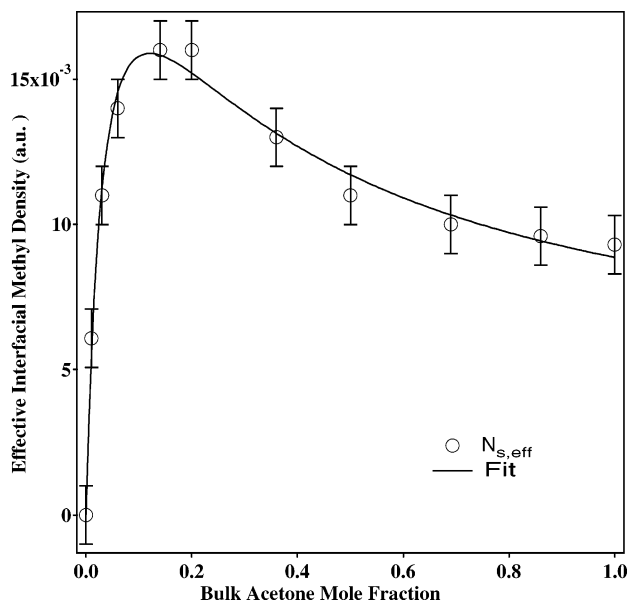


Figure 2. $N_{s,\text{eff}}$ as a function of bulk acetone mole fraction. The solid line is the fit with eq 14.

ordered top molecular layer. This can be achieved only through forming an antiparallel second adsorption layer, which shall cancel the SFG field from the first layer and thus reduce the $N_{s,\text{eff}}$ measured as the actual number of interfacial acetone molecules increases with increase of adsorption from the bulk liquid.

Lin and Shen et al. suggested previously in their MD simulation that for pure acetone the interfacial acetone molecules tend to have antiparallel orientation in the nearest neighbor statistics.²⁹ They also pointed out that recent X-ray diffraction studies on crystalline acetone at low-temperature had shown antiparallel layered structure,⁷⁰ and MD simulation in bulk acetone had also shown antiparallel arrangement in the nearest neighbor statistics.^{71,72} Lin and Shen then concluded that the vapor/pure acetone interface could be highly ordered and crystal-like, i.e., with antiparallel layered interface structure.²⁹ MD simulations have also shown antiparallel dimer formation in pure acetone liquid.⁶⁴

Since we have determined that the interface is well ordered throughout the low and high concentration ranges, it is clear that the forming of the antiparallel layer structure with increasing second layer adsorption should be the only possible explanation of the $N_{s,\text{eff}}$ drop with increasing bulk acetone concentration. Therefore, the SFG-VS measurement reported here on the vapor/acetone–water mixture interface not only provides the first direct experimental evidence supporting the highly ordered and crystal-like physical picture for the pure acetone interface but also indicates that this antiparallel layer interface structure forms gradually with the increase of the adsorption from the bulk acetone solution.

This antiparallel layered structure may not have a full antiparallel second layer, for $N_{s,\text{eff}}$ does not go to zero at higher concentration. Otherwise, the SFG-VS signal should have gone to zero when the second layer had fully formed. Thus, we propose a double-layer adsorption model (DAM) for the adsorption of acetone molecule to its vapor/aqueous solution interface. In this model, an adsorbed second layer gradually forms with an antiparallel structure, and it contributes negatively to the total SFG field. Therefore, we write

$$N_{s,\text{eff}} = N_s^{\text{max}}(\Theta - p\sigma) \quad (11)$$

TABLE 5: Fitting Results of Figure 2 with Eq 14^a

N_s^{max} (a.u.)	p	K_1	$\Delta G_{\text{ads},1}^\circ$	K_2	$\Delta G_{\text{ads},2}^\circ$
0.028 ± 0.007	0.69 ± 0.07	25 ± 9	-1.9 ± 0.2	5 ± 2	-0.9 ± 0.2

^a The unit for $\Delta G_{\text{ads},1}^\circ$ and $\Delta G_{\text{ads},2}^\circ$ is kcal/mol.

in which Θ is the first layer coverage and σ the second layer coverage, p ($-1 \leq p \leq 1$) is a proportional constant representing the efficiency for the second layer cancellation ($0 \leq p \leq 1$) or enhancement ($-1 \leq p \leq 0$), and N_s^{max} is the effective interfacial density for a full first layer coverage.

The Langmuir isotherm has provided the simplest treatment on adsorption of weakly interacting species to a surface.⁴ We denote the adsorption equilibrium constants as K_1 and K_2 , respectively. Because the second layer adsorption has to follow the first layer adsorption, simple derivation using the Langmuir isotherm as given in the physical chemistry textbooks⁴ shows

$$\Theta = \frac{K_1 x}{1 - x + K_1 x} \quad (12)$$

$$\sigma = \frac{K_2 x \Theta}{1 - x + K_2 x} \quad (13)$$

$$N_{s,\text{eff}} = N_s^{\text{max}} \frac{K_1 x}{1 - x + K_1 x} \left(1 - \frac{p K_2 x}{1 - x + K_2 x} \right) \quad (14)$$

Here one should notice that the expression of Θ in eq 12 differs from the ordinary Langmuir isotherm,⁴ which uses 1 in the denominator instead of $1 - x$. This is because when using the Langmuir isotherm to describe adsorption from dilute solution where x is usually much smaller than 1, $1 - x$ can be generally replaced with 1. However, for high bulk concentrations, such approximation is no longer valid.⁷³

Equation 14 gives a good fit for $N_{s,\text{eff}}$ vs acetone bulk mole fraction x , as shown by the solid line in Figure 2. Through the K_1 and K_2 values the adsorption free energy for the first and second layer could be obtained according to $\Delta G_{\text{ads},i}^\circ = -RT \ln K_i$. The results are listed in Table 5. In addition to using the Langmuir isotherm, we also tested the Frumkin isotherm which includes a treatment on the increasing interactions between the adsorbed molecules as the interface coverage Θ and σ increases.⁴ It is clear that when a single layer adsorption is considered, the Frumkin isotherm cannot predict any decrease of $N_{s,\text{eff}}$ at higher bulk acetone concentration. So it is clear that a DAM has to be included for Frumkin adsorption isotherm. With DAM, Frumkin works just as well as the simple Langmuir and produces very close fitting parameters for N_s^{max} , p , and $\Delta G_{\text{ads},1}^\circ$ and $\Delta G_{\text{ads},2}^\circ$, and a very small interaction energy term at full coverage. This means that the Langmuir treatment is good enough to describe the problem. This is also in agreement with our hypothesis above that interfacial acetone molecules assume orientation to minimize the lateral repulsive interactions between the neighboring acetone molecules. So no Frumkin correction term is necessary, and simple Langmuir isotherm is good enough here.

The coverage Θ and σ are calculated and listed in Table 4. They are also plotted against the bulk mole fraction in Figure 3. The value $p = 0.69 \pm 0.07$ falls into the range $0 \leq p \leq 1$ as we expected above. The free energy of adsorption for the first acetone layer is $\Delta G_{\text{ads},1}^\circ = -1.9 \pm 0.2$ kcal/mol. This value is well above the thermalization energy $kT = 0.59$ kcal/mol at the ambient temperature 295 °K. However, $\Delta G_{\text{ads},2}^\circ = -0.9 \pm 0.2$ kcal/mol compares to the thermalization energy kT . This suggests that the second layer cannot be as well ordered as the

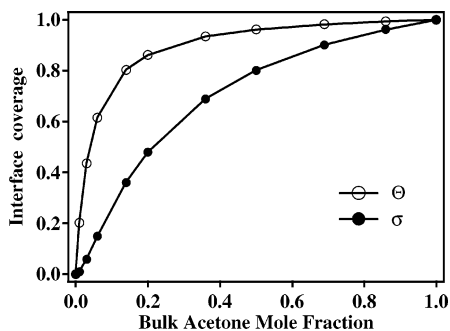


Figure 3. Interfacial coverage for the first and second layers.

first layer, which is consistent with the fact that p is less than unity. However, we also want to point out that the second layer is not to be very disordered, because the continuously decreasing D value with increasing acetone bulk mole fraction indicates a good ordered structure within the double layer structure including the second layer. Because $\Delta G_{\text{ads},1}^{\circ} > \Delta G_{\text{ads},2}^{\circ}$, Θ should always be larger than σ until both reach full coverage as the bulk becomes pure acetone. The difference between $\Delta G_{\text{ads},1}^{\circ}$ and $\Delta G_{\text{ads},2}^{\circ}$ is clearly shown in the Θ and σ values as in Figure 3. When the slope $p^* \partial \sigma / \partial x$ begins exceeding $\partial \Theta / \partial x$, $N_{\text{eff}}^{\text{max}}$ starts dropping. The bigger the $\Delta G_{\text{ads},2}^{\circ}$ value, the earlier the drop starts.

Comparison of $\Delta G_{\text{ads},1}^{\circ}$ and $\Delta G_{\text{ads},2}^{\circ}$ values with the adsorption free energy obtained with other methods provides interesting clues for understanding energetics in the Gibbs adsorption layers. Irving Langmuir's 1917 classical paper on the fundamental properties of liquids listed adsorption free energies for about 40 molecules at their aqueous solution interface from Traube's data obtained at the temperature of 15 °C,³ among which the value for acetone is -2.17 kcal/mol. It is known that at higher temperature the adsorption free energy should be smaller, therefore, this value is in good agreement with the $\Delta G_{\text{ads},1}^{\circ} = -1.9 \pm 0.2$ kcal/mol at 22 °C. Furthermore, Langmuir pointed out in his paper that "A theory of surface tension is now proposed in which the structure of the surface layer of atoms is regarded as the principal factor in determining the surface tension (or rather surface energy) of liquids. This theory is supported in the most remarkable way by all available published data on the surface tension of organic liquids." Since from our DAM the second layer is more disordered than the first layer, it is easy to see that the first layer adsorption should be the major contributor to the surface energy. Therefore, this quantitative agreement between the adsorption free energies cannot be treated as accidental.

However, we do not want to overstate the quantitative agreement between $\Delta G_{\text{ads},1}^{\circ}$ and the Langmuir's adsorption free energy value. From the surface tension data for the acetone–water mixture in the major handbooks,^{74,75} we calculated the adsorption free energy at 20 °C and found mixed results ranging from -1.8 kcal/mol, -2.0 kcal/mol, -2.9 kcal/mol to -3.0 kcal/mol. We also performed surface tension measurement on acetone–water mixture interfaces, and it gave an adsorption free energy of -2.8 ± 0.1 kcal/mol. If we consider the concept that the interface free energies are additive,^{4,76} then both the first and second layers contribute to the surface tension. Therefore, we have $\Delta G_{\text{ads},1}^{\circ} + \Delta G_{\text{ads},2}^{\circ} = -2.8 \pm 0.2$ kcal/mol, and this value matches perfectly with the surface tension value from our surface tension data. However, provided with so many different adsorption free energy values from data in the literature, even though we intend to believe, we are still not certain whether the value we measured with surface tension data is more accurate than the rest values from others. Notwithstand-

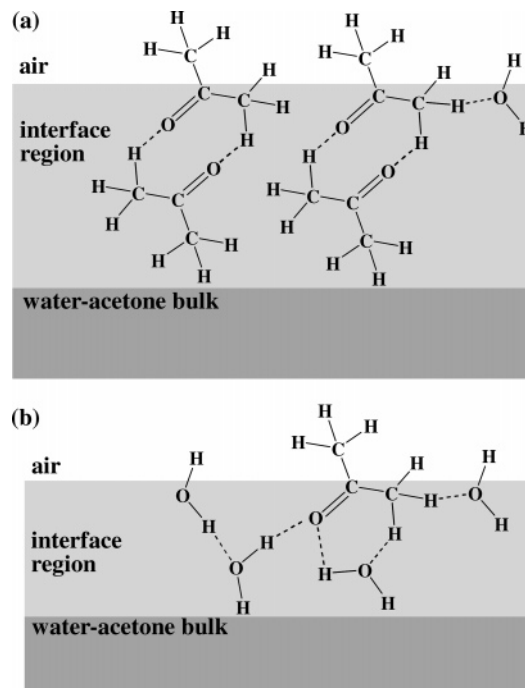


Figure 4. Schematic illustration of the possible structures for the vapor/acetone–water mixture interface. (a) Higher bulk concentration with interface dimer formation. (b) Lower bulk concentration before dimer formation. The dotted lines represents possible hydrogen bonds.

ing these uncertainties, it is reasonable to conclude that the first adsorption layer contributed most significantly to the surface tension. Nevertheless, this two layer structure is very intriguing, and further investigation is certainly necessary to better address this problem.

Furthermore, since the double layer interface structure is driven by either dipole or by hydrogen bonding interactions, and both interactions require certain preferred molecular orientations, an ordered third layer is not expected to form. The possible interface structures are schematically illustrated in Figure 4. First, the molecules in the third layer can interact only with the CH_3 groups that point down from the second layer. Since CH_3 does not have a strong dipole moment, it has an orientation not preferred to form a hydrogen bond from molecules below; it also blocks interaction with the $\text{C}=\text{O}$ group in the second layer, so the attractive interaction between the third layer and the second layer should be much weaker than that between the first two layers. Second, since $\Delta G_{\text{ads},2}^{\circ} = -0.9 \pm 0.2$ kcal/mol is already not much above kT at room temperature, if a $\Delta G_{\text{ads},3}^{\circ}$ could mean anything, it has to be much smaller, and the adsorption should be fully randomized by the thermalization. A direct educt from this fact is that the interface consists only two layers, with the first layer well ordered, the second partially ordered, and with the third layer fully thermalized as part of the bulk liquid. Therefore, the thickness of the interface is not more than two molecular layers. Experiments and theoretical simulation have persistently given very thin interface thickness for vapor/liquid and liquid/liquid interfaces.^{10,19,77,78} For example, X-ray reflectivity measurements and MD simulation give a thickness or interface roughness of 3.2 and 3.45 Å, respectively, for the air/water interface.^{10,19,77} The direct structural information obtained with SFG-VS studies as demonstrated here provides new insight to the description of the interface thickness problem.

Consequently, it would be very interesting to perform SFG-VS measurements at lower and higher temperatures. Since $\Delta G_{\text{ads},1}^{\circ}$ is well above kT , we expect the first layer ordering

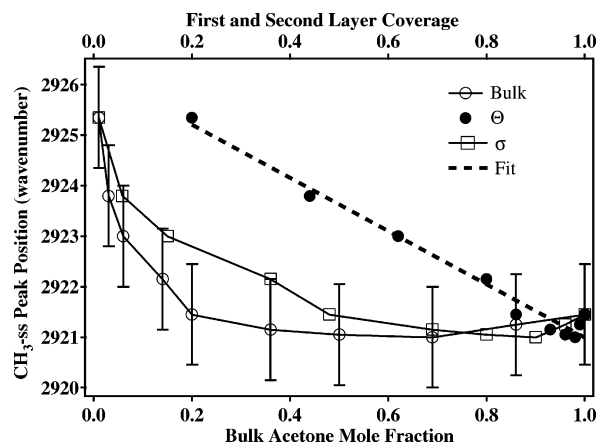


Figure 5. CH₃-ss peak position as a function of bulk acetone mole fraction, first and second layer coverage. The dashed line is a linear line fit. The solid lines are connection between neighboring points.

shall not be affected significantly with changing temperature in a certainly wide range. While $\Delta G_{\text{ads},2}^\circ$ is much closer to kT , therefore, the second layer structure should be affected significantly by changing temperature. We thus expect to see that the degree of drop of $N_{\text{s,eff}}$ should become more pronounced at lower temperature and less pronounced at higher temperature. Since this double layer structure is “crystal-like” as called by Lin and Shen et al., we also expect that dipolar liquids with higher melting point than acetone might show larger drop of $N_{\text{s,eff}}$ for their aqueous solution interface than that for acetone at the same temperature. For *tert*-butyl alcohol, which has a much higher melting point than acetone, we did observe an about 80% drop of the SFG-VS signal with increasing concentration at room temperature. However, not all the dipolar liquids can form the antiparallel double layer interface structure. It has been known that there is no significant SFG-VS signal drop for the air/neat water interface when temperature is increased from 10 to 80 °C.³⁰ This might be attributable to the fact that the dipole moment of the interfacial water molecule is nearly parallel to the interface;^{19,30} therefore, an antiparallel double layer structure for the air/water interface is geometrically against the forming of any tetrahedral hydrogen network structure.

3.2.1. Vibrational Spectra Peak Red-Shift and Segregation at the Interface. Structural information in the adsorbed layers can also be inferred from the SFG-VS spectral peak shift as shown in Figure 5, where the spectral shift is plotted against the bulk acetone mole fraction, first layer coverage Θ , and the second layer coverage σ , respectively. There is a clear linear relationship between the spectral red-shift with Θ , but no such relationship between the shift and the bulk mole fraction or σ . Therefore, the spectral shift is directly related to the formation of the first layer. We surmise that this fact suggests at least following two possibilities: (a) the continuously changing lateral interactions between acetone molecules in the first interface layer are responsible for this shift; (b) the interface consists of more than one spectroscopically different species, i.e., the interface is with segregated islands of clusters or aggregations coexisting with “free” acetone molecules, and their relative concentration is linearly dependent on the surface coverage Θ .

Recently, Allen et al. reported a similar red-shift for the CH₃-ss mode with an SFG-VS study on vapor/methanol–water interface, as well as with Raman spectral measurement for bulk methanol aqueous solution.⁵⁷ They also found a good linear correlation between this red-shift with the interface coverage of methanol molecules obtained from surface tension data. They attributed such red-shift to the changing hydrogen-bonding

configurations with increasing methanol concentration. However, with the knowledge of the antiparallel double layer interface structure, the interpretation may be different.

The vapor/methanol–water mixture interface also has an antiparallel double layer structure. Using the PNA technique in SFG-VS, we also studied the vapor/methanol–water mixture interface recently.^{45,79,80} With direct measurement of CH₃ orientation, we concluded that there is also a well-ordered first layer and a double-layer adsorption structure at the interface. There is also a linear relationship between the SFG-VS peak red-shift and the first layer coverage Θ . Therefore, the red-shift is not due to the formation of the second layer of methanol or acetone molecules, which should substitute the water molecules and change the hydrogen bonding between the molecules in the second layer and the methanol or acetone molecules in the first layer. This suggests that there might be different mechanisms for the red-shift in the interface SFG spectra from that in the bulk Raman spectrum. It is hard for one to define or understand a continuously changing lateral interaction between the methanol molecules in the bulk solution as in the interface layer, because methanol molecules are not aligned or ordered as are those at the interface. So the Raman shift in the bulk solution may not be explained by the lateral interactions that is absent in the bulk solution.

It is known that simple alcohols such as methanol and ethanol were reported to show cluster or segregation structures in their aqueous mixtures.⁸¹ A MD simulation by Klein et al. on the vapor/liquid interface of a 0.1 M ethanol–water solution observed segregation of ethanol at the interface.⁸² These all suggest that the interface may be with segregated clusters or islands, and they may be responsible for the SFG red-shift at the interface region. Similarly, with the same red-shift trend, the acetone–water mixture interface may also have segregated clusters or island structure. More experimental and theoretical studies are certainly needed to further address this issue.

The double layered interface structure was suggested by Saykally et al. for vapor/pure methanol interface from EXAFS absorption spectroscopy study on liquid methanol jet surface.¹² Our SFG-VS study on the vapor/methanol–water interface also supports this picture.^{79,80} In addition to methanol, we have carefully studied ethanol, acetonitrile, and *tert*-butyl alcohol aqueous mixture interfaces in our laboratory. For these systems, the SFG-VS intensities all drop at higher bulk concentration. This phenomenon was reported for ethanol and acetonitrile previously, but the interpretations varied.^{57–60} With the help of the PNA method to determine the orientational changes in the Gibbs adsorption layer, we can also determine the existence of the double layer structure at these interfaces, and their adsorption free energies were obtained.⁷⁹ We will report these results soon. Comparison of these results shall be very interesting and important for detailed understanding of the interactions and mechanisms determining the structure, conformation, and energetics of these liquid mixture interfaces. It seems to us that even though not all liquid mixture interfaces would form such double layered structures, it is quite a general phenomenon for interfaces of polar liquids at their interfaces and aqueous solution interfaces. The DAM model and Langmuir isotherm treatment of the problem presented in this report should be a useful tool to unravel the mysteries about the Gibbs interface layers.

It is interesting to note that a phenomenon called surface freezing was reported for liquid long-chain normal alkanes,⁸³ as well as long chain alcohols.^{84,85} This phenomenon shows about a 3 °K increase of the melting point for the surface layer than that of the bulk. Even though the causes were in debate,⁸⁶

it is sure that it is caused by chain interactions instead of dipolar or hydrogen bonding interactions. The ordered double layer structure we observed for polar liquids and liquid mixtures could also be considered a new kind of surface freezing phenomenon, driven by specific dipolar or hydrogen bonding interactions at the interface. Observation of such a surface freezing effect for the pure acetone interface is surprising, because its bulk melting point is at 179 °K, i.e., −94 °C. We have discussed elsewhere that this “freezing” of the vapor/acetone interface has to be dynamic with a lifetime that may be as short as one tenth of a microsecond.⁴⁹ However, as temperature drops, this surface “freezing” might persist for much longer time, and it may implicate new mechanisms for phenomena such as interface induced condensation and phase transition. Earlier we have excluded the possibility for a surface induced third layer formation at room temperature for acetone. But weaker interactions, such as van der Waals interactions, between the better ordered second layer and the layers beneath may cause some new phenomena at lower temperature at least when the system temperature is lowered closer to its melting point. The depth of the surface zone of a liquid could be much more complicated as has been speculated for many decades.^{87,88} Even though all these now are just hypotheses and intellectual guesses, we expect that future investigations may be able to provide new evidence and answers.

4. Conclusions

We have studied the SFG-VS spectra of the stretching mode of the CH₃ group of acetone molecules at the vapor/acetone–water mixture interface. With the polarization null angle (PNA) method, we are able to accurately measure the orientation and orientational change of acetone molecules at the vapor/liquid interface. At the vapor/aqueous solution interface, the acetone molecule has its C=O group point into the bulk phase, with one CH₃ group pointing up and another CH₃ group pointing into the bulk phase. This orientational configuration changes slightly with acetone bulk concentration. From the knowledge of molecular orientation, we then identified the orientationally independent effective surface density $N_{s,eff}$ for the interface CH₃ group. The drop of $N_{s,eff}$ at higher acetone bulk concentration helped us to identify the antiparallel double layer interface structure of the acetone molecules adsorbed to the interface. This antiparallel double layer structure is induced by dipolar interactions or specific hydrogen bonding interactions between two acetone molecules. The adsorption free energy of the two layers are also obtained through a double layer model and Langmuir isotherm. The adsorption free energies thus obtained are -1.9 ± 0.2 kcal/mol and -0.9 ± 0.2 kcal/mol for the first and second layers, respectively. We then conclude that the vapor/acetone–water interface is only two layers thick, with the first layer well ordered and the second layer less well ordered. These results provided direct microscopic structural evidence for understanding the Gibbs adsorption layers and the fundamental properties of the liquid interfaces.

These detailed studies on vapor/acetone–water interface with SFG-VS have provided us unexpected information on the structure and energetics on the Gibbs adsorption layers at this interface. It is a good demonstration of the capability of the recently developed quantitative analysis methods in SFG-VS, especially the PNA method. In our future reports, we shall present detailed studies on the interface of aqueous solution of methanol, ethanol, acetonitrile and DMSO and many other liquids with these newly developed techniques in SFG-VS. These efforts shall generate deep understanding and shall greatly

enhance our knowledge on structure, conformation, energetics and dynamics in the Gibbs adsorption layers at the liquid interfaces in general. The technique demonstrated in this report can also be applied to study other molecular interfaces in chemistry, biology, and material sciences.

Acknowledgment. H.F.W. thanks the Chinese Academy of Sciences (the Hundred Talent Program starting fund), the Natural Science Foundation of China (NSFC No.20274055, No.20425309), and the Chinese Ministry of Science and Technology (MOST No. G1999075305) for support. H.F.W. thanks Na Ji at Ron Shen's group for suggestion on testing of the Frumkin isotherm. H.F.W. thanks Professor Jianbin Huang's laboratory at Peking University for assistance on measuring surface tensions of acetone–water solution interfaces.

References and Notes

- (1) Gibbs, J. W. “On the Equilibrium of Heterogeneous Substances”, *Connecticut Academy Transactions*, **1875–1876**, 3, 108–248; **1877–1878**, 3, 343–524.
- (2) Gibbs, J. W. *The Scientific Papers of J. Willard Gibbs: Thermodynamics*, Ox Bow Press: Woodbridge, CT, 1993.
- (3) Langmuir, I. *J. Am. Chem. Soc.* **1917**, 39, 1848–1906.
- (4) Adamson, A. W.; Gast, A. P. *Physical Chemistry of Surfaces*, 6th ed.; Wiley-Interscience: New York, 1997.
- (5) Evans, D. F.; Wennerström, H. *The Colloidal Domain: Where Physics, Chemistry, Biology, and Technology Meet*, 2nd ed.; Wiley-VCH: New York, 1999.
- (6) Myers, D. *Surfaces, Interfaces, and Colloids: Principles and Applications*; VCH: New York, 1999; Chapter 8.1.
- (7) Eiselthal, K. B. *Acc. Chem. Res.* **1993**, 26, 636–643, and references therein.
- (8) Miranda, P.; Shen, Y. R. *J. Phys. Chem. B* **1999**, 103, 3292 and references therein.
- (9) Garrett, B. C. *Science* **2004**, 303, 1146.
- (10) Braslau, A.; Deutsch, M.; Pershan, P. S.; Weiss, A. H.; Als-Nielsen, J.; Bohr, J. *Phys. Rev. Lett.* **1985**, 54, 114–117.
- (11) Kaganer, V. M.; Möhwald, H.; Dutta, P. *Rev. Mod. Phys.* **1999**, 71, 779–819.
- (12) Wilson, K. R.; Schaller, R. D.; Co, D. T.; Saykally, R. J. *J. Chem. Phys.* **2002**, 117, 7738–7744.
- (13) Thomas, R. K.; Penfold, J. *Curr. Opin. Colloid Interface Sci.* **1996**, 1, 1.
- (14) Penfold, J. *Rep. Prog. Phys.* **2001**, 64, 777–814.
- (15) Eiselthal, K. B. *Chem. Rev.* **1996**, 96, 1343–1360 and references therein.
- (16) Croxton, C. A. *Statistical Mechanics of the Liquid Surfaces*; Wiley: New York, 1980.
- (17) Safran, S. A. *Statistical Thermodynamics of Surfaces, Interfaces, and Membranes*; Addison-Wesley: Reading MA, 1994.
- (18) Smit, B. In *Computer Simulation in Chemical Physics*; Allen, M. P., Tildesley, D. J., Eds.; Kluwer Academic Publishers: Dordrecht, 1993; pp 173–210.
- (19) Townsend, R. M.; Rice, S. A. *J. Chem. Phys.* **1991**, 94, 2207–2218.
- (20) Klein, M. L. *J. Chem. Soc., Faraday Trans.* **1992**, 88, 1701.
- (21) Benjamin, I. *Chem. Rev.* **1996**, 96, 1449–1475.
- (22) Benjamin, I. *Annu. Rev. Phys. Chem.* **1997**, 48, 407–451.
- (23) Kuo, I. F. W.; Mundy, C. J. *Science* **2004**, 303, 658–660.
- (24) Duque, D.; Vega, L. F. *J. Chem. Phys.* **2004**, 121, 8611–8617.
- (25) Richmond, G. L. *Annu. Rev. Phys. Chem.* **2001**, 52, 357–389 and references therein.
- (26) Benjamin, I. *Phys. Rev. Lett.* **1994**, 73, 2083–2086.
- (27) Scatena, L. F.; Brown, M. G.; Richmond, G. L. *Science* **2001**, 292, 908–912.
- (28) Rossky, P. J. *Nature* **2002**, 419, 889–890.
- (29) Yeh, Y. L.; Zhang, C.; Held, H.; Mebel, A. M.; Wei, X.; Lin, S. X.; Shen, Y. R. *J. Chem. Phys.* **2001**, 114, 1837–1843.
- (30) Du, Q.; Superfine, R.; Freysz, E.; Shen, Y. R. *Phys. Rev. Lett.* **1993**, 70(15), 2313–2316.
- (31) Adamson, A. W.; Gast, A. P. *Physical Chemistry of Surfaces*, 6th ed.; Wiley-Interscience: New York, 1997; Chapter III-2.
- (32) Shen, Y. R. *Annu. Rev. Phys. Chem.* **1989**, 40, 327–350.
- (33) Shen, Y. R. *Appl. Phys. B* **1999**, 68, 295–300.
- (34) Bain, C. D. *J. Chem. Soc., Faraday Trans.* **1995**, 91, 1281–1296.
- (35) Zhuang, X.; Miranda, P. B.; Kim, D.; Shen, Y. R. *Phys. Rev. B* **1999**, 59, 12632–12640.

- (36) Heinz, T. F.; Tom, H. W. K.; Shen, Y. R. *Phys. Rev. A* **1983**, 28, 1883.
- (37) Zhang, T. G.; Zhang, C. H.; Wong, G. K. *J. Opt. Soc. Am. B* **1990**, 7(6), 902–907.
- (38) Zhang, D.; Gutow, J.; Eienthal, K. B. *J. Phys. Chem.* **1994**, 98, 13729–13734.
- (39) Hirose, C.; Akamatsu, N.; Domen, K. *J. Chem. Phys.* **1992**, 96(2), 997–1004.
- (40) Hirose, C.; Yamamoto, H.; Akamatsu, N.; Domen, K. *J. Phys. Chem.* **1993**, 97, 10064–10069.
- (41) Watanabe, N.; Yamamoto, H.; Wada, A.; Domen, K.; Hirose, C. *Spectrochim. Acta A* **1994**, 50(8,9), 1529–1537.
- (42) Lambert, A. G.; Neivandt, D. J.; Briggs, A. M.; Usadi, E. W.; Davies, P. B. *J. Phys. Chem. B* **2002**, 106, 5461–5469.
- (43) McGall, S. J.; Davies, P. B.; Neivandt, N. J. *J. Phys. Chem. B* **2004**, 108, 16030–16039.
- (44) Rao, Y.; Tao, Y. S.; Wang, H. F. *J. Chem. Phys.* **2003**, 119, 5226–5236.
- (45) (a) Lu, R.; Gan, W.; Wang, H. F. *Chin. Sci. Bull.* **2003**, 48(20), 2183–2187. (b) Lu, R.; Gan, W.; Wang, H. F. *Chin. Sci. Bull.* **2004**, 49(9), 899.
- (46) Lu, R.; Gan, W.; Wu, B. H.; Chen, H.; Wang, H. F. *J. Phys. Chem. B* **2004**, 108, 7297–7306.
- (47) Wang, H. F. *Chin. J. Chem. Phys. (English)* **2004**, 17, 362–368.
- (48) Lu, R.; Gan, W.; Wu, B. H.; Chen, H.; Wang, H. F., submitted to *J. Phys. Chem. B*.
- (49) Chen, H.; Gan, W.; Wu, B. H.; Zhang, Z.; Wang, H. F., submitted to *Chem. Phys. Lett.*
- (50) Snyder, R. G.; Aljibury, A. L.; Strauss, H. L.; Casal, H. L.; Murphy, W. F. *J. Chem. Phys.* **1984**, 81(12), 5352–5360.
- (51) Snyder, R. G.; Scherer, J. R. *J. Chem. Phys.* **1979**, 71, 3221–3228.
- (52) Snyder, R. G.; Strauss, H. L.; Elliger, C. A. *J. Phys. Chem.* **1982**, 86, 5145–5150.
- (53) MacPhail, R. A.; Strauss, H. L.; Snyder, R. G.; Elliger, C. A. *J. Phys. Chem.* **1984**, 88, 334–341.
- (54) Snyder, R. G.; Hsu, S. L.; Krimm, S. *Spectrochim. Acta A* **1978**, 34, 395–406.
- (55) Ye, P. X.; Shen, Y. R. *Phys. Rev. B* **1983**, 28, 4288–4294.
- (56) Allen, H. C.; Raymond, E. A.; Richmond, G. L. *Curr. Opin. Colloid Interface Sci.* **2000**, 5, 74–80.
- (57) Ma, G.; Allen, H. C. *J. Phys. Chem. B* **2003**, 107, 6343–6349.
- (58) Huang, J. Y.; Wu, M. H. *Phys. Rev. E* **1994**, 50, 3737–3746.
- (59) Kim, J.; Chou, K. C.; Somorjai, G. A. *J. Phys. Chem. B* **2003**, 107, 1592–1596.
- (60) Sung, J.; Park, K.; Kim, D. *J. Korean Phys. Soc.* **2004**, 44, 1394–1398.
- (61) (a) Tyrode, E.; Johnson, C. M.; Baldelli, S.; Leygraf, C.; Rutland, M. W. *J. Phys. Chem. B* **2004**, 109, 321–328. (b) Johnson, C. M.; Tyrode, E.; Baldelli, S.; Leygraf, C.; Rutland, M. W. *J. Phys. Chem. B* **2004**, 109, 329–341.
- (62) Simpson, G. J.; Rowlen, K. L. *J. Am. Chem. Soc.* **1999**, 121, 2635.
- (63) Simpson, G. J.; Rowlen, K. L. *Acc. Chem. Res.* **2000**, 33, 781–789.
- (64) Hermida-Ramón, J. M.; Ríos, M. A. *J. Phys. Chem. A* **1998**, 102, 2594–2602.
- (65) Stanners, C. D.; Du, Q.; Chin, R. P.; Cremer, P.; Somorjai, G. A.; Shen, Y. R. *Chem. Phys. Lett.* **1995**, 232, 407–413.
- (66) Wang, J.; Paszti, Z.; Even, M. A.; Chen, Z. *J. Am. Chem. Soc.* **2002**, 124, 7016–7023.
- (67) Superfine, R.; Huang, J. Y.; Shen, Y. R. *Phys. Rev. Lett.* **1991**, 66(8), 1066–1069.
- (68) Wolfrum, K.; Graener, H.; Laubereau, A. *Chem. Phys. Lett.* **1993**, 213, 41–46.
- (69) (a) Simpson, G. J.; Rowlen, K. L. *Anal. Chem.* **2000**, 72, 3399–3406. (b) Simpson, G. J.; Rowlen, K. L. *Anal. Chem.* **2000**, 72, 3407–3411.
- (70) (a) Allan, D. R.; Clark, S. J.; Ibberson, R. M.; Parsons, S.; Pulham, C. R.; Sawyer, L. *Chem. Commun.* **1999**(8), 751. (b) Allen, F. H.; Baalham, C. A.; Lommerse, J. P. M.; Raithby, P. R. *Acta Crystallogr., Sect. B* **1998**, 54, 320.
- (71) Jedlovsky, P.; Palinkas, G. *Mol. Phys.* **1995**, 84, 217.
- (72) Hermida-Ramón, J. M.; Ríos, M. A. *J. Phys. Chem. A* **1998**, 102, 2594.
- (73) Wang, H. F.; Yan, E. C. Y.; Liu, Y.; Eienthal, K. B. *J. Phys. Chem. B* **1998**, 102, 4446–4450.
- (74) *Landolt-Börnstein IV-16: Surface Tension of Pure Liquids and Binary Liquid Mixtures*; Lechner, M. D., Ed.; Springer: Berlin, 1997.
- (75) *The Physico-chemical Constants of Binary Systems in Concentrated Solutions*; Timmermans, J., Ed.; Wiley-Interscience, New York, 1960; Vol. 4.
- (76) Shaw, D. J. *Introduction to Colloid & Surface Chemistry*, 4th ed.; Butterworth Heinemann: Oxford, 1992; Chapter 4.
- (77) Braslau, A.; Pershan, P. S.; Swislow, G.; Ocko, B. M.; Als-Nielsen, J. *Phys. Rev. A* **1988**, 38, 2457–2470.
- (78) Nicolas, J. P.; de Souza, N. R. *J. Chem. Phys.* **2004**, 120, 2464–2469.
- (79) Chen, H.; Gan, W.; Lu, R.; Guo, Y.; Wang, H. F. *J. Phys. Chem. B* **2005**, 109, 8064–8075.
- (80) Chen, H. *Structure and Adsorption of Acetone and Methanol at Vapor/Liquid Interfaces by Sum Frequency Generation Vibrational Spectroscopy*; Ph.D. Dissertation, Institute of Chemistry, the Chinese Academy of Sciences, 2004, No. 200118003202812, Defence date: June 24, 2004.
- (81) Dixit, S.; Crain, J.; Poon, W. C. K.; Finney, J. L.; Soper, A. K. *Nature* **2002**, 416, 829–832.
- (82) Tarek, M.; Tobias, D. J.; Klein, M. L. *J. Chem. Soc., Faraday Trans.* **1996**, 92, 559.
- (83) Wu, X. Z.; Ocko, B. M.; Sirota, E. B.; Sinha, S. K.; Deutsch, M.; Cao, B. H.; Kim, M. W. *Science* **1993**, 261, 1018–1021.
- (84) Deutsch, M.; Wu, Z. X.; Sirota, E. B.; Sinha, S. K.; Ocko, B. M.; Magnussen, O. M. *Europhys. Lett.* **1995**, 30, 283.
- (85) Gang, O.; Wu, Z. X.; Ocko, B. M.; Sirota, E. B.; Deutsch, M. *Phys. Rev. E* **1998**, 58, 6086.
- (86) (a) Sirota, E. B.; Wu, X. Z.; Ocko, B. M.; Deutsch, M. *Phys. Rev. Lett.* **1997**, 79, 531. (b) Tkachenko, A.; Rabin, Y. *Phys. Rev. Lett.* **1997**, 79, 532.
- (87) Henniker, J. C. *Rev. Mod. Phys.* **1949**, 21, 322–341.
- (88) Hardy, W. B. *Proc. R. Soc. London* **1912**, A86, 610–635.